Journal of Computation Physics and Earth Science
ISSN: 2776-2521 (online)
Volume 5, Number 2, February 2026, Page 189 - 201
https://journal.physan.org/index.php/jocpes/index

Fault Mapping of the Central Aceh Segment of the Sumatran Fault as an Extension of the Great Sumatran Fault (GSF) Using Gravity Analysis

Qisthi Mursyida[1], Muhamad Syirojudin[2]
[1]Undergraduate Program in Geophysics (STMKG)
[2]Indonesian Agency for Meteorology, Climatology, and Geophysics (BMKG)

Article Info

Article history:

Received December 27, 2025
Revised March 6, 2026
Accepted March 6, 2026

Keywords:

Gravity
First Horizontal Derivative (FHD)
Second Vertical Derivative (SVD)
Central Aceh Segment

A B S T R A C T

Aceh is known as one of the most tectonically active regions in Indonesia with a relatively high level of seismicity. One of the active zones is the Central Aceh Segment, which forms part of the Sumatra Fault as an extension of the Great Sumatran Fault. This study aims to identify the distribution and characteristics of fault zones and types in the Central Aceh Segment using gravity data from GGMplus. The analysis was carried out by applying the First Horizontal Derivative (FHD) and Second Vertical Derivative (SVD) methods. The results indicate significant lateral density contrasts that delineate the presence of a major fault and several secondary fault structures within the study area. Interpretation of SVD values along several profiles suggests that many of the inferred structures exhibit reverse fault characteristics, with some indications of normal faults. These features are interpreted as secondary deformation structures that may develop within a strike-slip fault under localized transpressional or transtensional stress regimes. Subsurface geological modelling along profiles AA′–BB′, BB′–CC′, and EE′–FF′ shows variations in rock density that highlight zones of high-density distribution.

Corresponden Author:

Qisthi Mursyida,
Undergraduate Program in Geophysics (STMKG)
Tangerang, Indonesia
Email: mursyidaq@gmail.com

1. INTRODUCTION

The Sumatran (Great Sumatran Fault) is an important geological structure that contributes significantly to the high level of seismic activity in Indonesia [1]. Due to its location at the convergence of three major tectonic plates, the Indo-Australian, Eurasian, and Pacific plates. Indonesia is highly vulnerable to earthquakes. The Great Sumatran Fault extends approximately 1900 km from Lampung in the south to the Andaman region in the north and is divided into twenty fault segments, each with distinct characteristics [2].

The Aceh Fault represents the northernmost segment of the GSF and has a total length of approximately 250 km [3]. It plays an important role in right lateral strike-slip motion resulting from the oblique convergence between the Indo-Australian Plate and the Eurasian Plate with a convergence rate of about 70 mm/year along the Sunda subduction zone [4]. According to the Indonesian National Earthquake Hazard Map, the Aceh Fault is divided into three segments: the North Aceh Segment, the Central Aceh Segment, and the South Aceh Segment. As the central portion of the Aceh Fault System, the Central Aceh Segment serves as a structural link between the North and South Aceh segments. Deformation within this segment may therefore influence other segments along the fault zone. Historical records indicate moderate seismic activity along the Aceh Fault, particularly within the Central Aceh Segment, over the past 170 years; however, no major earthquakes have been recorded [5]. This condition suggests the potential accumulation of significant tectonic stress in the region.

This study employs gravity analysis to identify the Central Aceh Segment. Based on Newton's law of gravitation, [6] stated that the gravitational force between two objects is directly proportional to their masses

and inversely proportional to the square of the distance between them. This principle forms the basis of gravity analysis in geophysics, particularly for fault identification. The gravity method was selected because it can reveal subsurface structural features through variations in gravity anomalies caused by differences in rock density [7]. Residual and regional gravity anomaly patterns in the study area were analyzed using secondary gravity data from GGMPlus and TOPEX. Furthermore, First Horizontal Derivative (FHD) and Second Vertical Derivative (SVD) analyses were applied to enhance the delineation of fault locations and geometries [8].

2. RESEARCH METHOD

The fault trace crossing the Central Aceh Segment within the study area is shown on the topographic map in Figure 1. The topographic map illustrates significant elevation variations, with lowland areas and coastal waters located to the west and north of the Aceh region. This study area is defined by longitude coordinates ranging from 95.9° to 96.3° and latitude coordinates from 4.7° to 5.0°, which were subsequently analyzed to obtain Free Air Anomaly (FAA) data, as shown in Figure 2. Gravity data from GGMPlus were used in this study with a spatial resolution of 7.2 arc-seconds (220 m).

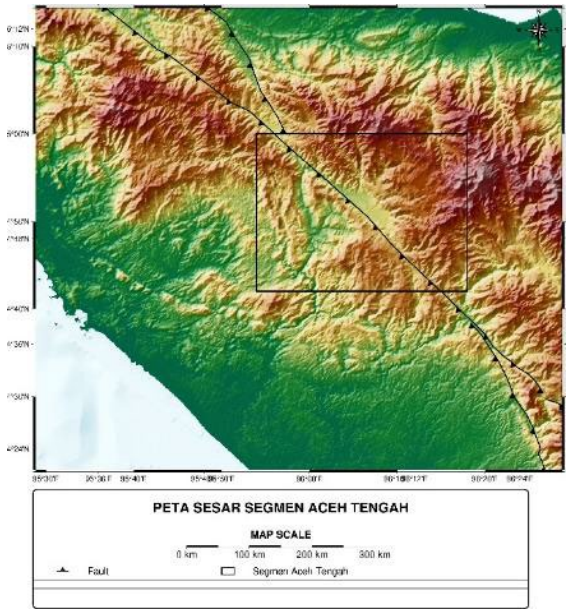

Fig. 1. Map of the Study Area

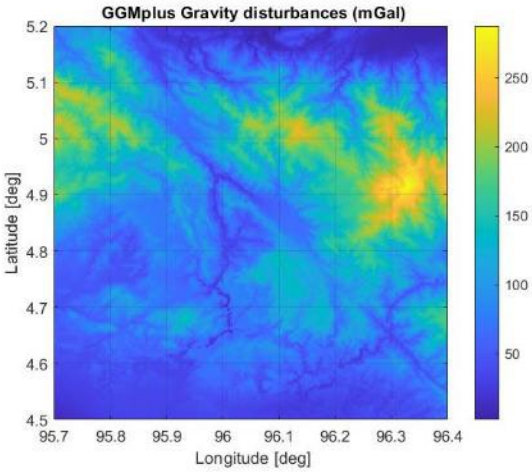

Fig. 2. Free Air Anomaly (FAA) Map of the Study Area

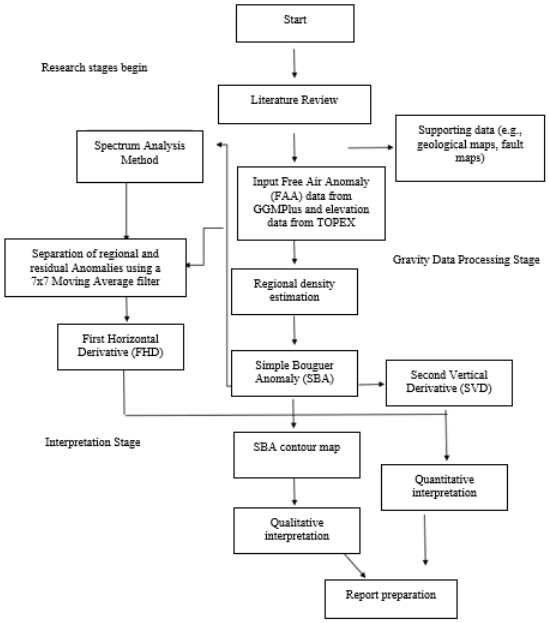

Fig. 3. Flowchart of Gravity Data Processing

Figure 3 illustrates the stages of gravity data processing applied in this study. The first stage involves determining the estimated regional density value for the boundary of the study area. The Parasnis method was employed to perform this calculation, as it is commonly used to estimate the average rock density. According to [9], the determination of rock density requires elevation data (h), Free Air Anomaly (FAA), field corrections, and Bouguer corrections.

Subsequently, Microsoft Excel was used to process the FAA data in order to obtain the average density value, Bouguer correction, and Simple Bouguer Anomaly (SBA). The FAA values were derived from data that had undergone automatic corrections, including tidal, drift, and latitude corrections. The FAA values can be calculated using equation (1):

$$FAA = 0.04192 \times \rho_a \times h + L_g \quad (1)$$

Where:

FAA : Free air anomaly (mGal)
ρ_a : Average air density (gr/cm^3)
h : Elevation (m)
L_g : Latitude gravity correction (mGal)

The next step is to determine the Simple Bouguer Anomaly (SBA) by subtracting the Bouguer correction from FAA values. This procedure is performed based on Equation (2) to calculate the mass effect between the observation point and the Earth's surface [10]. Equation (3) can then be used to obtain the SBA values.

$$BC = 0.04192 \times \rho_a \times h \quad (2)$$

$$SBA = FAA - BC \quad (3)$$

Where:

BC : Bouguer correction (mGal)
ρ_a : Average air density (gr/cm^3)
h : Elevation (m)
SBA : Simple bouguer anomaly (SBA)
FAA : Free air anomaly (mGal)

Surfer software was used to process the SBA values in this study. Because the topographic variation in the Central Aceh Segment is relatively stable, the SBA values are considered sufficient for analysis, although some areas may exhibit elevation differences related to geological structures. The next step involved determining the regional anomaly using a second order polynomial method with a low pass filter, which aims to remove high frequency components and retain only low frequency data. This process highlights the regional anomaly, which reflects large scale density patterns in greater detail. Subsequently, the corresponding SBA values were subtracted from the regional anomaly to obtain the residual anomaly. These two anomalies provide a clearer representation of subsurface patterns based on depth and density distribution [11].

Furthermore, the SBA data were processed using a 7x7 moving average filter to generate residual anomalies that facilitate the interpretation of subsurface structures in the study area. The moving average filter separates regional and residual anomalies by emphasizing low frequency signals in the Bouguer Anomaly, which are then used to derive the regional anomaly. The residual anomaly is subsequently obtained by subtracting the regional anomaly from the total Bouguer anomaly, as expressed in equation (4):

$$\Delta g_{Residual} = \Delta g_{Bouguer} - \Delta g_{Regional} \quad (4)$$

Where:

$\Delta g_{Residual}$: Residual anomaly (mGal)
$\Delta g_{Bouguer}$: Bouguer anomaly (mGal)
$\Delta g_{Regional}$: Regional anomaly (mGal)

To identify fault structures, the previously determined regional anomaly was further analyzed using First Horizontal Derivative (FHD) and Second Vertical Derivative (SVD) techniques. SVD analysis is applied to interpret the sources of gravity anomalies and to determine fault mechanism [12]. Meanwhile, FHD analysis enables the identification of horizontal density contrast boundaries. Zones exhibiting the highest FHD values are interpreted as potential fault locations. The inferred fault locations correspond to zones where the maximum values of the FHD coincide with the zero contour of the SVD response.

In this study, the Henderson and Zietz matrix filter (Table 1) was selected for SVD analysis. SVD is a derivative of FHD and is used to identify fault mechanism as well as to validate the presence of fault structures. Fault locations are identified when the FHD values reach a maximum while the corresponding SVD values approach zero.

Table 1. Henderson and Zietz (1949) matrix used as a 7x7 SVD filter

Henderson and Zietz (1949)				
0	0	-0.0838	0	0
0	+1.0000	-2.6667	+1.0000	0
-0.0838	-2.6667	17.0000	-2.667	-0.0838
0	+1.0000	-2.6667	+1.0000	0
0	0	-0.0838	0	0

The criteria presented in equation (5) can then be applied to determine the faulting mechanism based on the SVD values [9].

$$\left|\frac{\partial^2 \Delta g}{\partial z^2}\right|_{min} < \left|\frac{\partial^2 \Delta g}{\partial z^2}\right|_{max} \quad normal\ fault \tag{5}$$

$$\left|\frac{\partial^2 \Delta g}{\partial z^2}\right|_{min} > \left|\frac{\partial^2 \Delta g}{\partial z^2}\right|_{max} \quad reverse\ fault \tag{6}$$

$$\left|\frac{\partial^2 \Delta g}{\partial z^2}\right|_{min} \approx \left|\frac{\partial^2 \Delta g}{\partial z^2}\right|_{max} \quad strike-slip\ fault \tag{7}$$

3. RESULTS AND DISCUSSION

3.1. Average Density

The average rock density value obtained is required for mapping the Central Aceh Segment fault. In this study, the average rock density was calculated using the Parasnis method. The average rock density in the Central Aceh Segment is 2.5343 g/cm^{3}.

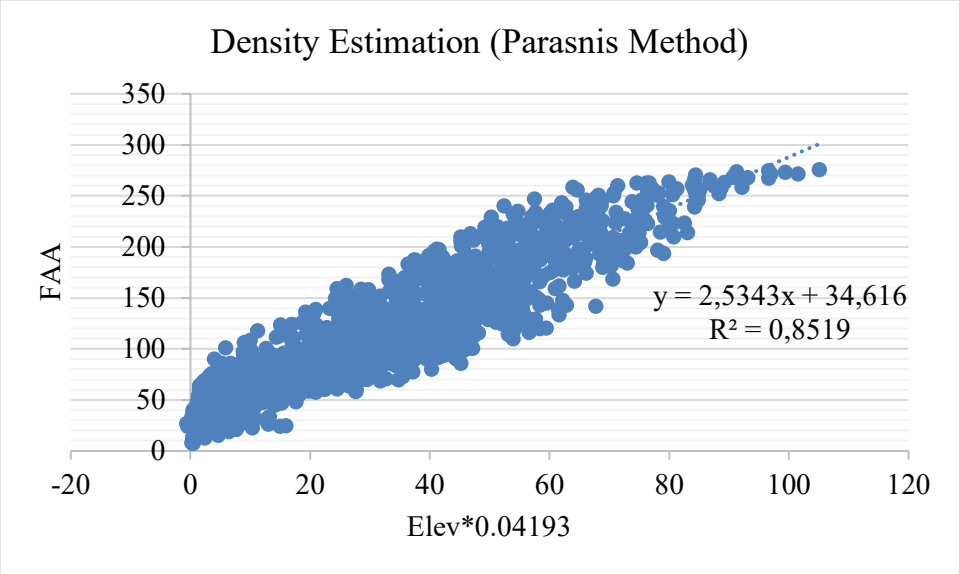

Fig. 4. Determination of average rock density using the Parasnis method

The Central Aceh Segment has an average density of 2.5343 g/cm3. As stated by [13], rocks can be classified into sedimentary, igneous, and metamorphic types based on their density ranges and average density values for each rock type. Figure 4 shows that several rock types may dominate the Central Aceh region with a density of approximately 2.5343 g/cm3. Based on standard rock density tables, this density range may indicate the presence of sedimentary rocks such as limestone (1.93-2.90 Mg/m3), igneous rocks such as granite (2.55-2.75 Mg/m3), and andesite (2.40-2.80 Mg/m3).

Jenis batuan	Rentang densitas(Mg/m³)	Rata-rata(Mg/m³)
Sedimentary rocks		
Alluvium	1.96 – 2.00	1.98
Clay	1.63 – 2.60	2.21
Gravel	1.70 – 2.40	2.00
Loess	1.40 – 1.93	1.64
Silt	1.80 – 2.20	1.93
Soil	1.20 – 2.40	1.92
Sand	1.70 – 2.30	2.00
Sandstone	1.61 – 2.76	2.35
Shale	1.77 – 3.20	2.40
Limestone	1.93 – 2.90	2.55
Dolomite	2.28 – 2.90	2.70
Chalk	1.53 – 2.60	2.01
Halite	2.10 – 2.60	2.22
Glacier ice	0.88 – 0.92	0.90
Igneous rocks		
Rhyolite	2.35 – 2.70	2.52
Granite	2.50 – 2.81	2.64
Andesite	2.40 – 2.80	2.61
Syenite	2.60 – 2.95	2.77
Basalt	2.70 – 3.30	2.99
Gabbro	2.70 – 3.50	3.03
Metamorphic rocks		
Schist	2.39 – 2.90	2.64
Gneiss	2.59 – 3.00	2.80
Phylite	2.68 – 2.80	2.74
Slate	2.70 – 2.90	2.79
Granulite	2.52 – 2.73	2.65
Amphibolite	2.90 – 3.04	2.96
Eclogite	3.20 – 3.54	3.37

Fig. 5. Determination of average rock density [13]

3.2. Simple Bouguer Anomaly (SBA)

The Simple Bouguer Anomaly (SBA) values were calculated using an average density of 2.5343 g/cm3. The SBA values on the map range from -35 mGal to 105 mGal, as shown in Figure 6. The minimum SBA value of -35 mGal occurs in the dark blue area located in the upper right part of the map, while the maximum SBA value of 105 mGal is observed in the bright red area around the upper left portion of the map.

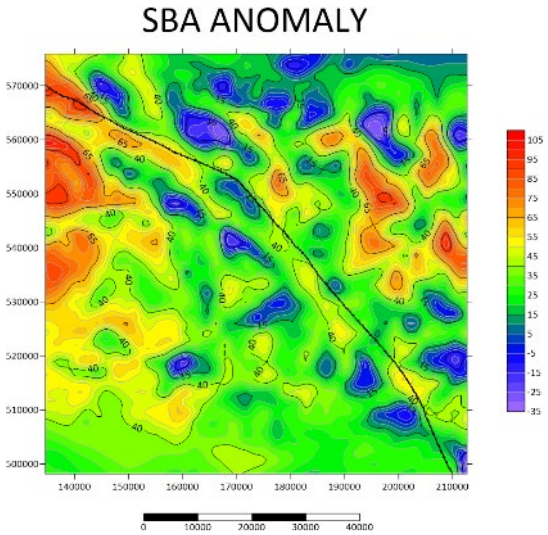

Fig. 6. Simple Bouguer Anomaly (SBA) map of the suspected fault zone in the study area

3.3. Spectral Analysis

Spectral analysis was performed to separate regional and residual gravity anomalies within the study area. The analysis was conducted using the radially averaged power spectrum method to determine the cut-off frequency separating regional and residual anomaly components. The identified cut-off frequency was subsequently used to define the moving window size for the moving average filter applied in the regional-residual separation. Prior to conducting spectral analysis, the SBA data were examined by constructing several profiles across the study area. Two horizontal profiles and three vertical profiles were constructed to provide a more comprehensive representation of gravity anomalies within the Central Aceh Segment. This approach enables the identification of gravity anomaly patterns based on depth and lateral variations in subsurface mass distribution. The three vertical profiles illustrate variations in gravity anomaly characteristics along the north-south direction, while the two horizontal profiles depict lateral distributions along the east-west direction, as shown in Figure 7.

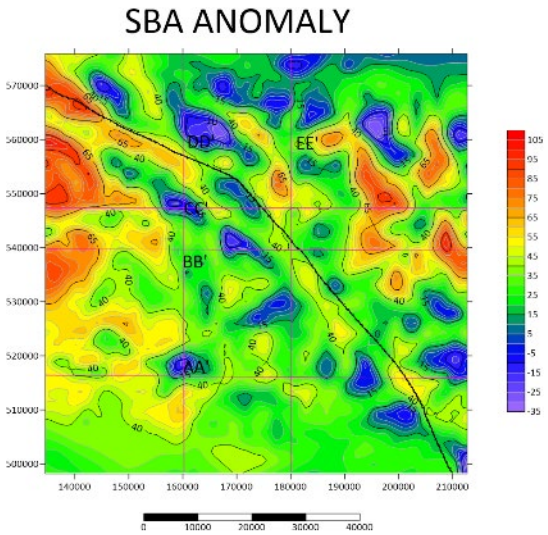

Fig. 7. SBA map with five profiles

The spectral method is applied to separate regional and residual anomalies from gravity data. Residual anomalies represent local sources, such as shallow intrusions or sedimentary basins, whereas regional anomalies reflect large scale density variations, including those associated with the deeper crust.

Table 2. Depth of regional and residual zones, cut-off frequency, and predicted window width derived from spectral analysis

	Regional Zone	Residual Zone	Cut-Off Frequency (k)	Predicted Window Width (n)
Profile AA’	146.08 m	13.499 m	0.0036956	7.728091
Profile BB’	177.95 m	72.995 m	0.0036956	7.728091
Profile CC’	175.25 m	19.994 m	0.0036956	7.728091
Profile DD’	154.16 m	55.081 m	0.0038465	7.424914
Profile EE’	144.2 m	23.959 m	0.0038465	7.424914

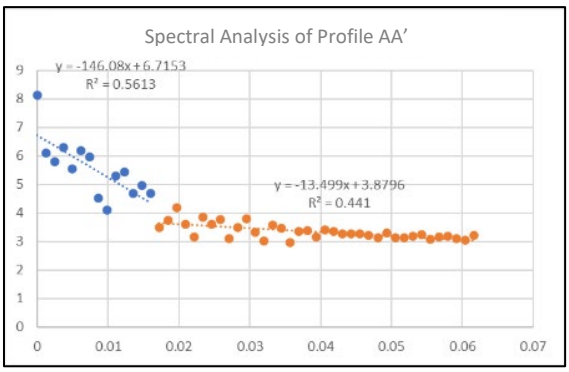

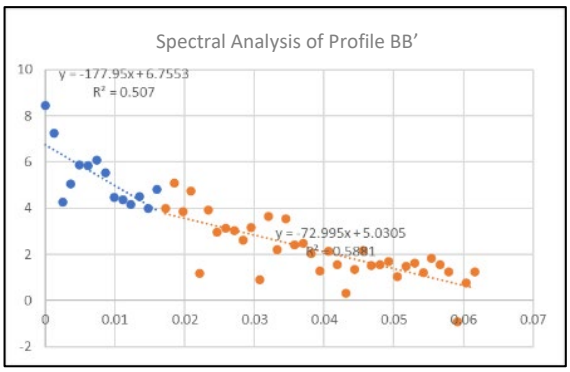

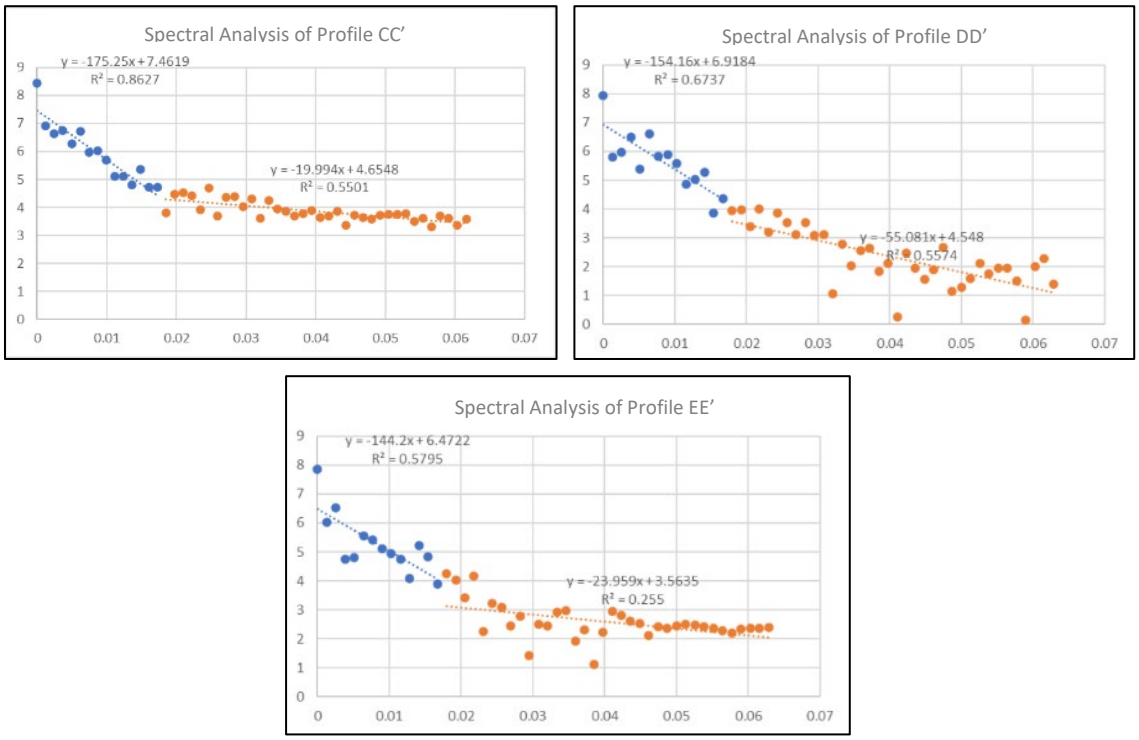

Fig. 8. Spectral analysis graphs of the five profiles

3.4. Separation of Regional and Residual Anomalies

After defining the regional and residual zones based on the results of spectral analysis, the separation of regional and residual anomaly values was carried out to identify the presence of fault structures. Regional anomaly values can be used to map geological structures associated with relatively low seismic activity. Therefore, the regional anomaly was utilized for mapping the Central Aceh Segmen Fault after obtaining the SBA value.

The regional anomaly was calculated using the moving average method, which smooths data values over a specified area (a 7x7 grid was applied in this study). Once the regional anomaly was obtained, the residual anomaly was calculated by subtracting the regional anomaly from the total gravity data. The residual anomaly aids in identifying shallow geological structures, such as active faults within the Central Aceh Segment. This method reduce noise in gravity data, thereby enhancing the visibility of regional geological structures at specific depths.

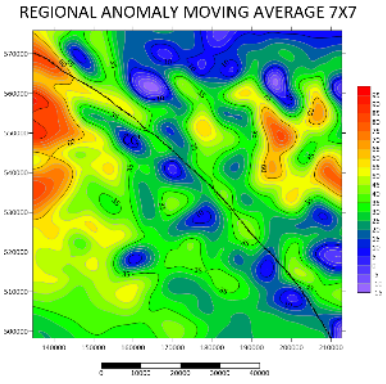

Fig. 9. Regional anomaly map

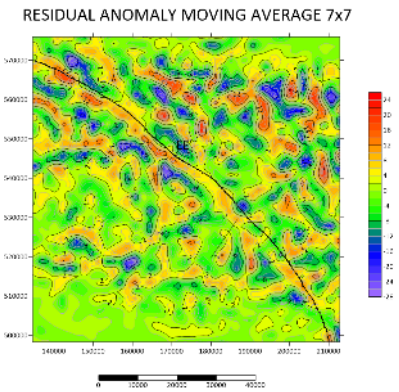

Fig. 10. Residual anomaly map

3.5. First Horizontal Derivative (FHD) and Second Vertical Derivative (SVD) Analysis

Figure 11 presents the 7x7 moving average anomaly map, which is characterized by the dominance of green to blue colors with value ranging from 0 to 95 mGal, indicating variations in rock density within the shallow subsurface layers. The black fault lines shown on both maps represent the main faults mapped by [14]. These faults reflect major tectonically active geological structures that play a significant role in the crustal deformation pattern of the region.

In this study, nine profiles were selected to analyze variations in gravity gradient patterns along the Central Aceh Segment. The FHD values, which are predominantly shown in green and yellow colors, are higher in areas closer to the fault traces identified by [14], indicating higher density materials. In contrast, lower FHD values are observed in areas farther from the fault lines, particularly in the southern part of the study area, suggesting the presence of lower density rocks.This result indicates a significant density contrast between the northern and southern regions of the Central Aceh Segment.

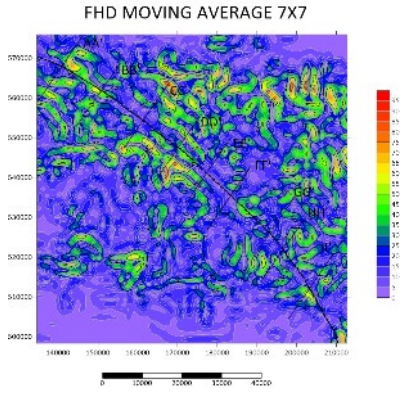

Fig. 11. FHD value map

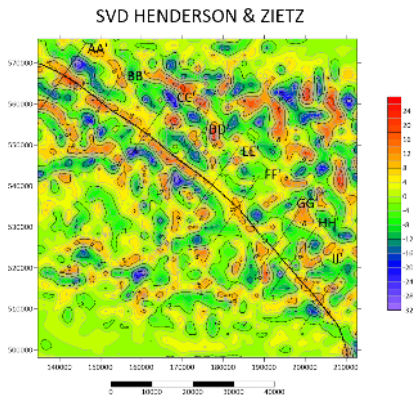

Fig. 12. SVD value map

Meanwhile, the SVD values shown in Figure 12 were used tp strengthen the gravity interpretation by emphasizing vertical gravity variations. Positive values on the map (red zones) indicate high density rocks, such as magmatic intrusions or hard igneous rocks (e.g., granite or basalt), whereas negative values (blue zones) represent low density rocks, such as unconsolidated sediments or weathered rocks. The black fault lines displayed on both maps represent the main faults mapped by the National Center for Earthquake Studies [14]. These faults reflect major tectonically active geological structures that play a significant role in crustal deformation patterns in the region. In this study, nine profiles were selected to analyze variations in gravity gradient patterns along the Central Aceh Segment.

3.6. Fault Type Determination

The results of the FHD and SVD profile analyses were used to determine the faulting mechanism. Based on the interpretation of the FHD and SVD maps, several areas exhibiting significant anomaly values were identified in the vicinity of the fault zone. Overall, the anomalies are more dominant in the western part of the study area, as indicated by the vertical lines shown in each profile plot.

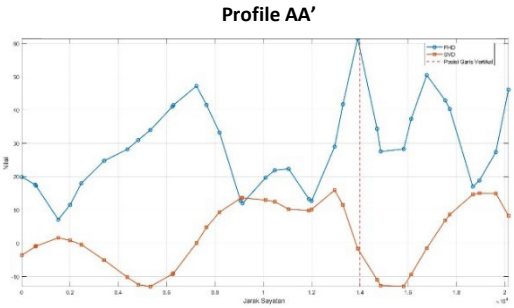

Fig. 13. Profile AA' plot

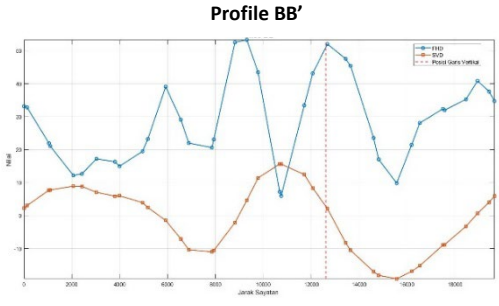

Fig. 14. Profile BB' plot

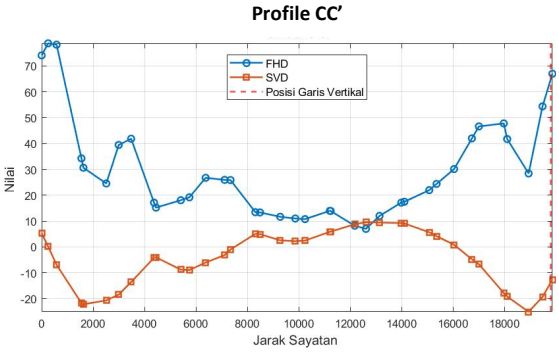

Fig. 15. Profile CC' plot

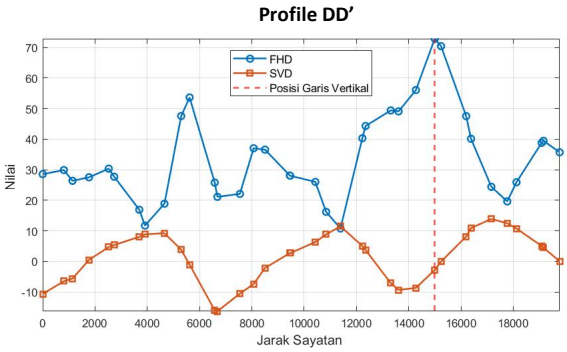

Fig. 16. Profile DD' plot

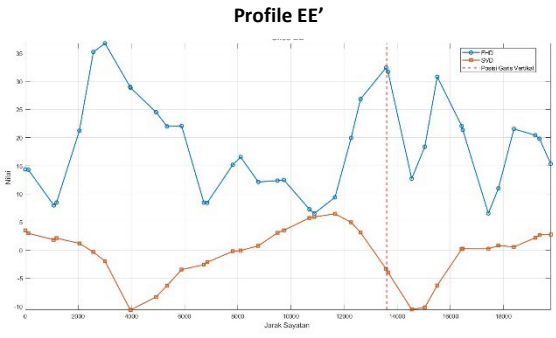

Fig. 17. Profile EE' plot

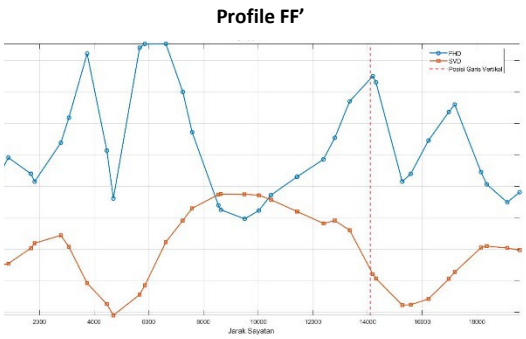

Fig. 18. Profile FF' plot

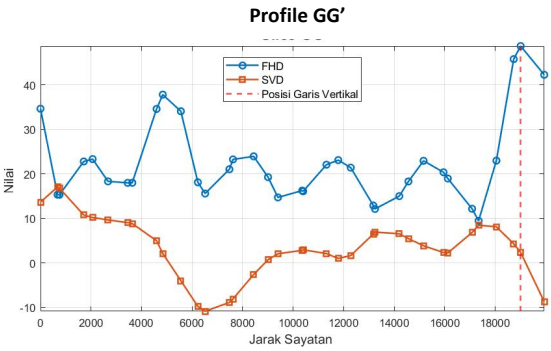

Fig. 19. Profile GG' plot

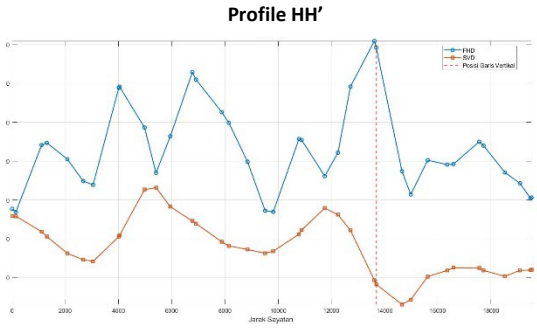

Fig. 20. Profile HH' plot

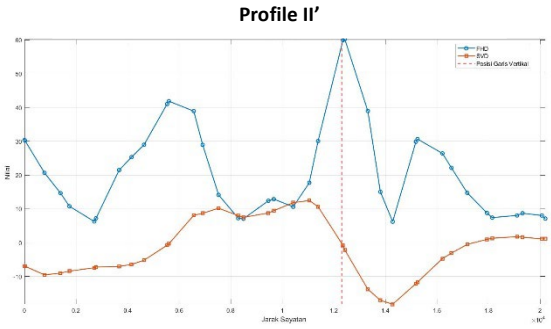

Fig. 21. Profile II' plot

The vertical lines from each profile were subsequently reinterpreted on the FHD and SVD maps. The red lines shown in Figures 22 and 23 represent the interpreted trace of the inferred fault, identified based on the results of the FHD and SVD analyses. These lines indicate locations where significant changes in gravity anomaly values occur, which commonly reflect major geological contacts such as faults. The inferred fault is interpreted to separate subsurface masses with contrasting densities, likely representing boundaries between

geological formations that have been displaced by tectonic activity. The continuity of the red lines across all profiles reflects the regional extent of the fault structure, indicating that his fault extends laterally and constitutes a dominant structural element within the geological framework of the Central Aceh Segment.

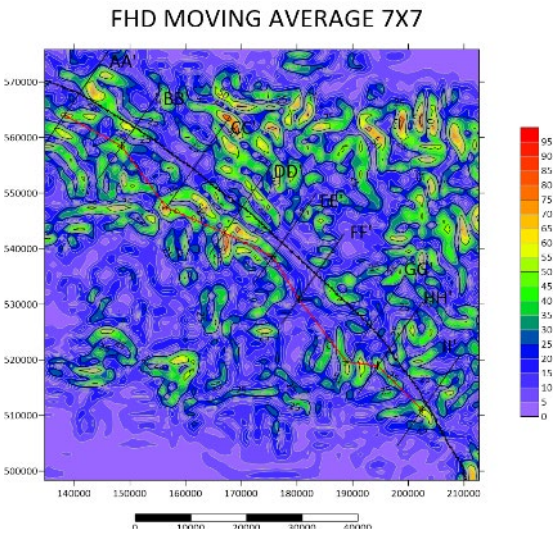

Fig. 22. FHD map with red lines indicating the inferred fault traces

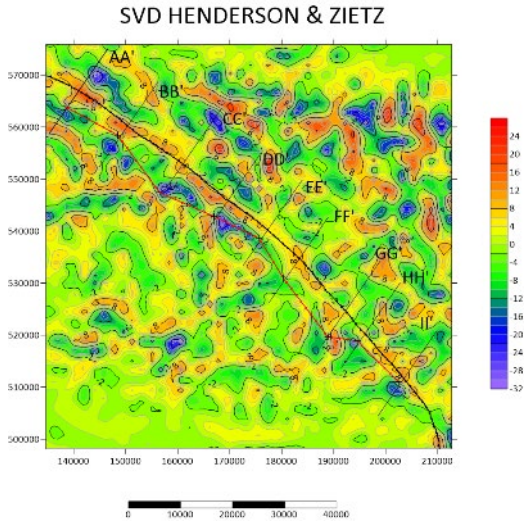

Fig. 23. SVD map with red lines indicating the inferred fault traces

The SVD analysis of nine profiles (AA', BB', CC', DD', EE', FF', GG', HH', and II') reveals significant patterns of lateral density variation. These variations are critical for interpreting the fault type analyzed in this study. Vertical lines identified in each profile indicate locations where the density gradient reaches minimum and maximum values. These vertical lines represent lateral density contrast boundaries, which suggest the presence of subsurface fault structures.

Table 3. Coordinates of density contrast boundaries and SVD value analysis

Profile	SVD Values		Fault Type
	Max	Min	
AA'	15.9535331194	-13.0035986565	Normal Fault
BB'	15.6510554835	-19.1467587229	Reverse Fault
CC'	9.58175155155	-25.1163248523	Reverse Fault
DD'	13.9040073916	-16.3071743018	Reverse Fault
EE'	6.46795543255	-10.624170777	Reverse Fault
FF'	8.78673984857	-10.475106417	Reverse Fault
GG'	17.0612422091	-10.8636700368	Normal Fault
HH'	13.1624224529	-16.8928254433	Normal Fault
II'	12.4525926134	-18.2321410379	Reverse Fault

Based on the SVD values and fault types interpreted in Table 3, most of the inferred fault traces in the Central Aceh Segment exhibit characteristics of reverse (thrust) faults. However, it should be noted that the Sumatran Fault is generally classified as a strike-slip fault by the [14]. Nevertheless, further analysis within [14] studies indicates that, in the deeper part of the accretionary prism, deformation zones in the form of arc-parallel reverse faults (backthrust) have developed, as observed in the Andaman Sea. Such backthrust structures are commonly associated with oblique convergence and transpressional tectonic regimes, where compressional components are locally accommodated within an overall strike-slip fault system. This mechanism allows reverse faulting to coexist with strike-slip deformation and may explain the dominance of thrust fault characteristics inferred from the SVD analysis in the Aceh Segment. In addition, strike-slip fault zones commonly develop secondary structures such as reverse or normal faults depending on the prevailing stress

regime. Under transpressional conditions, strike-slip deformation may generate positive flower structures characterized by reverse faulting, whereas transtensional regimes may produce negative flower structures associated with normal faulting [15]. Therefore, this explains the dominance of reverse fault observed in this study.

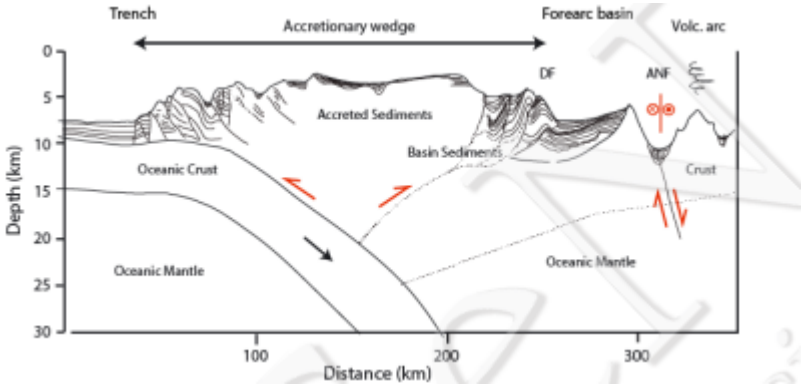

Fig. 24. Cross section of the Andaman subduction system showing the accretionary prism, forearc basin, and volcanic arc

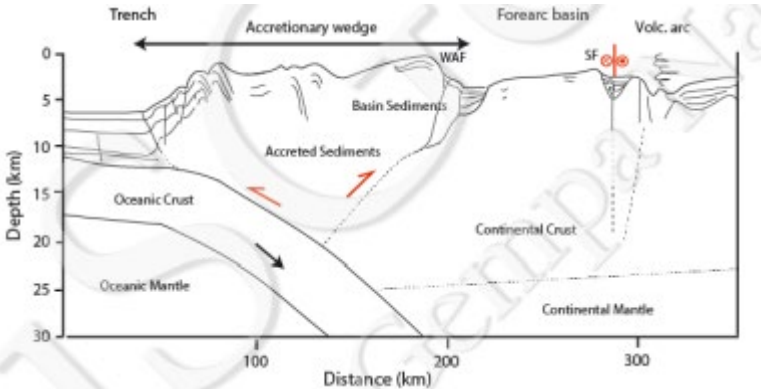

Fig. 25. Cross section of the Northern Sumatra subduction system showing the accretionary prism, forearc basin, and volcanic arc

In Aceh and its surrounding regions, a similar phenomenon can be observed, where arc-parallel reverse fault form boundaries between the accretionary prism and the forearc basin. Seismic and bathymetric data in this region support the presence of reverse faults as part of the tectonic deformation dynamics resulting from plate convergence. This zone serves as an important structural link between the Andaman Sea to the north and deformation zones in southern Sumatra.

3.7. Geological Modelling from Residual Anomalies

Red profile lines were again delineated as inferred fault traces in Figure 26, which require further analysis to better understand the subsurface conditions. The inferred fault trace exhibits a significant lateral density contrast, reflecting differences in the physical properties of rocks on either side of the fault as well as within its central zone. The three profiles (AA', BB', and CC') show consistent gravity anomaly patterns, indicating the presence of a fault in the central part of the study area (marked by a black line within the blue anomaly zone) in Figure 26.

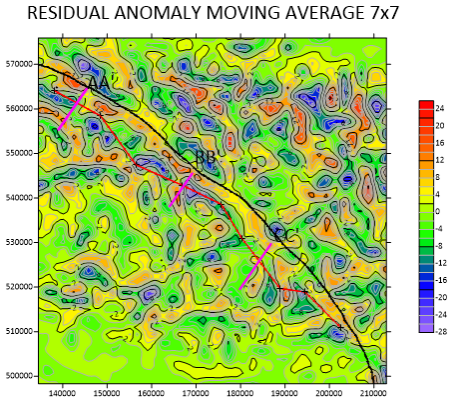

Fig. 26. Residual anomaly map of the Central Aceh Segment study area with red lines indicating the inferred fault traces

The main objective of this interpretation is to understand subsurface geological modelling, including density distribution, structural orientation, and their potential relationship with active faults, such as other segments of the Sumatran Fault as an extension of the Great Sumatran Fault (GSF). By utilizing residual anomaly data, local geological rock conditions can be effectively delineated.

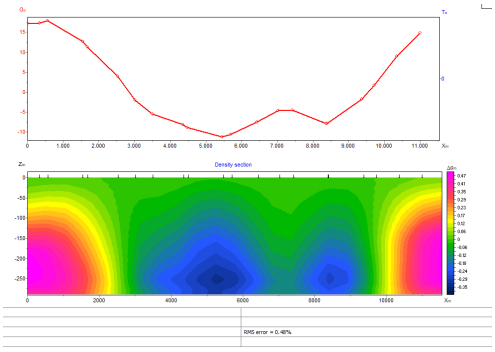

Fig. 27. Geological model along profile AA'

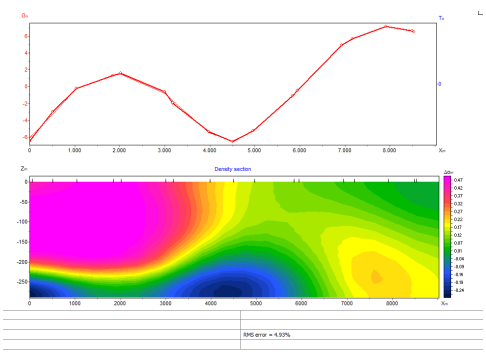

Fig. 28. Geological model along profile BB'

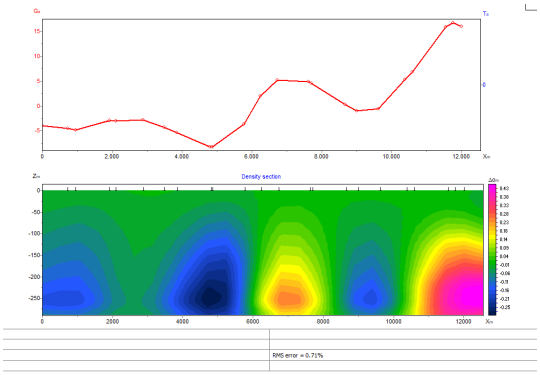

Fig. 29. Geological model along profile CC'

Along profile AA' in Figure 27, a significant change in gravity values is observed, with a zone of higher density material on one side and lower density material on the other. This contrast indicates a lithological difference that is most likely caused by faulting. Profile BB in Figure 28 further supports this interpretation, showing a sharp gravity gradient that reflect subsurface material displacement characteristic of geological faulting. A similar pattern is also evident along profile CC' in Figure 29, where asymmetric gravity anomaly patterns indicate displacement of subsurface layers. The consistency of anomaly patterns across these three profiles supports the interpretation that a fault is present in the central part of the study area, which likely a normal fault or a reverse fault.

4. CONCLUSION

The inferred fault traces indicate significant tectonic deformation patterns within the Central Aceh Segment, which are predominantly characterized as reverse faults based on the SVD analysis. This deformation

patterns are consistent with tectonic processes observed in the Andaman Sea, where arc-parallel reverse faults develop within the accretionary prism dynamics. These finding support the hypothesis that tectonic deformation in northern Sumatra, including the Aceh region, is tectonically connected to the Andaman subduction, reflecting the continuity of deformation zones from the Andaman Sea to Sumatra.

REFERENCE

[1] Y. Muhammad, A. Faisal, A. Yenny, Z. Muzakir, M. Abubakar, and I. Nazli, "Continuity of Great Sumatran fault in the marine area revealed by 3D inversion of gravity data," J. Teknol., vol. 83, no. 1, pp. 145–155, 2021, doi: 10.11113/jurnalteknologi.v83.14824.

[2] B. Munir, "Penggunaan Data Gempa dan Data Geologi Untuk Menganalisa Pola-Pola Sesar di Daratan Pulau Sumatra," p. 136, 2015.

[3] L. Y. Roodhiyah et al., "Interpretation of a 3D Magnetotellurics Model of the Aceh and Seulimeum Segments of the Sumatran Fault Zone," Appl. Sci., 2024.

[4] G. I. Marliyani et al., "Exploring Aceh Fault Zone for Slip Rates and Paleoseismic Trenching Potential along Sumatran Fault," Indones. J. Geogr., vol. 56, no. 1, pp. 138–148, 2024, doi: 10.22146/IJG.93456.

[5] A. K. Hady and G. I. Marliyani, Dr., "Updated Segmentation Model and Cumulative Offset Measurement of the Aceh Segment of the Sumatran Fault System in West Sumatra, Indonesia," J. Appl. Geol., vol. 5, no. 2, p. 84, 2021, doi: 10.22146/jag.56134.

[6] R. I. Hackney and W. E. Featherstone, "Geodetic versus geophysical perspectives of the 'gravity anomaly,'" Geophys. J. Int., vol. 154, no. 1, pp. 35–43, 2003, doi: 10.1046/j.1365-246X.2003.01941.x.

[7] M. Yanis, F. Abdullah, N. Zaini, and N. Ismail, "The northernmost part of the Great Sumatran Fault map and images derived from gravity anomaly," Acta Geophys., vol. 69, no. 3, pp. 795–807, 2021, doi: 10.1007/s11600-021-00567-9.

[8] N. A. Sunarto, Identifikasi Struktur Geologi Bawah Permukaan Berdasarkan Metode Second Vertical Derivative (SVD) Data Gravitasi di Kabupaten Bantul. 2021.

[9] Taufiquddin, "Identifikasi Struktur Bawah Permukaan daerah Potensi Panas Bumi Dengan Metode Gravity (Studi Kasus Di Daerah Sumber Air Panas Desa Lombang Kecamatan Batang-Batang Kabupaten Sumenep)," UIN Maulana Malik Ibrahim, pp. 1–100, 2014.

[10] K. Nozaki, "The generalized Bouguer anomaly," Earth, Planets Sp., vol. 58, no. 3, pp. 287–303, 2006, doi: 10.1186/BF03351925.

[11] I. Setiadi, C. Purwanto, D. Kusnida, and Y. Firdaus, "Interpretasi Geologi Bawah Permukaan Berdasarkan Analisis Data Gayaberat Menggunakan Filter Optimum Upward Continuation Dan Pemodelan 3D Inversi : (Studi Kasus: Cekungan Akimeugah Selatan, Laut Arafura)," J. Geol. Kelaut., vol. 17, no. 1, 2019, doi: 10.32693/jgk.17.1.2019.579.

[12] P. Sumintadireja, D. Dahrin, and H. Grandis, "A note on the use of the second vertical derivative (SVD) of gravity data with reference to Indonesian cases," J. Eng. Technol. Sci., vol. 50, no. 1, pp. 127–139, 2018, doi: 10.5614/j.eng.technol.sci.2018.50.1.9.

[13] W. M. Telford, L. P. Geldart, R. E. Sheriff, and A. Keys, D, "Applied Geophysics, Second Edition," Cambridge Univ. Press, 1990.

[14] P. S. G. Nasional, PETA SUMBER DAN BAHAYA GEMPA INDONESIA TAHUN 2017. 2017.

[15] K. Sieh and D. Natawidjaja, "Neotectonics of the Sumatran fault, Indonesia' Now," J. Geophys. Res., vol. 105, 2000.